pp 1109–1130. © Royal Aeronautical Society 2017
doi: 10.1017/aer.2017.49

Diagnostics of power setting sensor fault of gas turbine engines using genetic algorithm

Yi-Guang Li
i.y.li@cranfield.ac.uk
School of Aerospace, Transport and Manufacturing
Cranfield University
Cranfield, Bedford MK43 0AL
UK

ABSTRACT

Gas path diagnostics is one of the most effective condition monitoring techniques in supporting condition-based maintenance of gas turbines and improving availability and reducing maintenance costs of the engines. The techniques can be applied to the health monitoring of different gas path components and also gas path measurement sensors. One of the most important measurement sensors is that for the engine control, also called the power setting sensor, which is used by the engine control system to control the operation of gas turbine engines. In most of the published research so far, it is rarely mentioned that faults in such sensors have been tackled in either engine control or condition monitoring. The reality is that if such a sensor degrades and has a noticeable bias, it will result in a shift in engine operating condition and misleading diagnostic results.

In this paper, the phenomenon of a power-setting sensor fault has been discussed and a gas path diagnostic method based on a Genetic Algorithm (GA) has been proposed for the detection of power-setting sensor fault with and without the existence of engine component degradation and other gas path sensor faults. The developed method has been applied to the diagnostic analysis of a model aero turbofan engine in several case studies. The results show that the GA-based diagnostic method is able to detect and quantify the power-setting sensor fault effectively with the existence of single engine component degradation and single gas path sensor fault. An exceptional situation is that the power-setting sensor fault may not be distinguished from a component fault if both faults have the same fault signature. In addition, the measurement noise has small impact on prediction accuracy. As the GA-based method is computationally slow, it is only recommended for off-line applications. The introduced GA-based diagnostic method is generic so it can be applied to different gas turbine engines.

Keywords: Gas turbine; sensor; diagnostics; engine; genetic algorithm

Received 13 October 2016; revised 24 April 2017; accepted 3 May 2017; first published online 3 July 2017.
This paper will be presented at the ISABE 2017 Conference, 3-8 September 2017, Manchester, UK.

NOMENCLATURE

CFC	Component Fault Case
EF/η	isentropic efficiency
FC	Flow Capacity (kg/s)
m_f	fuel flow rate (kg/s)
P	total pressure (atm)
PCN	relative rotational speed (%)
PR	compressor Pressure Ratio
PSS	Power-Setting Sensor
SF	health parameter Scaling Factor
SFC	Sensor Fault Case
T	total temperature (°K)
TET	Turbine Entry Temperature (°K)
$\vec{x}$	health parameter vector
$\vec{y}$	ambient and power setting parameter vector
$\vec{z}$	measurement parameter vector
ε	average prediction errors

Subscripts

c	compressor
deg	degraded
B	burner
DH	Enthalpy Drop
FC	Flow Capacity
LPC/HPC	Low-/High-Pressure Compressor
LPT/HPT	Low-/High-Pressure Turbine
PR	Pressure Ratio
t	turbine

Superscripts

→	vector
^	predicted

1.0 INTRODUCTION

Degradation and fault may happen to both gas path components and sensors alike in gas turbine engines. Engine gas path component degradation may result in poor engine performance and eventual failure of entire engines, which will have significant economic consequences for gas turbine users. Gas path sensors are installed for engine control and condition monitoring. If degradation happens to sensors installed for condition monitoring only, it may result in misleading engine fault signatures (i.e., the deviation of gas path measurements) and misleading diagnostic results. If degradation happens to sensors installed for engine control or power setting, such as those for the measurement of engine exhaust temperature, shaft rotational speed or shaft power output, it will result in shifted engine performance, shifted gas path measurements and therefore misleading fault signatures and even complete failure of gas path diagnostic analysis.

Different gas turbine gas path diagnostic techniques have been developed in the past and comprehensive reviews of the technology have been provided by Li,[1] Singh[2] and Jaw[3]. Typical examples of gas path diagnostic techniques for gas turbines are gas path analysis and its derivatives,[4-9] neural network-based methods,[10-12] genetic algorithm-based methods,[13-15] fuzzy logic-based methods,[16-18] Bayesian belief network approaches,[19] diagnostics using transient measurements,[20-21] etc.

Most gas path sensors are used for condition monitoring purposes, some for safety control and one for engine control. The sensor used for engine control is one of the most important sensors and may be called the Power-Setting Sensor (PSS), and the corresponding parameter may be called the power-setting parameter. Gas path sensor fault diagnostics have been explored by many researchers using different methods, such as a Genetic Algorithm (GA) approach,[13] Artificial Neural Networks (ANN),[22-24] GPA,[8] pattern recognition,[25] Bayesian belief networks,[26] etc. These methods are able to detect gas path sensor faults, although they have different advantages and disadvantages. For example, the GA-based method is more robust than others but the computational load is higher; the ANN method is a computationally fast approach but needs a large number of training samples and long time for training; and the GPA methods use a moderate amount of computing time but may have convergence issues. However, the exploration of sensor fault diagnostics has been limited to gas path sensors except the power-setting sensor. In other words, it has been assumed implicitly so far that the power setting sensor has no fault. However, this sensor is so important that if it has a significant bias, it will result in a significant shift in engine performance and consequently may result in a complete failure of gas path diagnostic analysis. Initial investigation of this problem and a solution using artificial neural networks by the same research team was carried out and published in 2016[27].

This paper presents a novel GA-based gas path diagnostic approach for the diagnosis of engine power setting sensor fault with and without engine component and other gas path sensor degradations. The proposed new method was applied to a model aero turbofan engine to test the effectiveness of the method in several case studies. The results, discussions and conclusions are provided accordingly.

2.0 METHODOLOGY

2.1 Gas turbine performance and modelling

A gas turbine engine and its control system may be schematically shown in the upper part of Fig. 1. The thermodynamic behaviour of gas turbine engines may be mathematically represented by Equation (1)

$$\vec{z} = \boldsymbol{h}\left(\vec{x},\ \vec{y}\right) \tag{1}$$

where $\vec{z} \in R^N$ is the gas path measurement parameter vector and N is the number of the parameters, $\vec{x} \in R^M$ is the engine health parameter vector and M is the number of the parameters, $\vec{y} \in R^K$ is the ambient and power-setting parameter vector and K is the number

https://doi.org/10.1017/aer.2017.49 Published online by Cambridge University Press

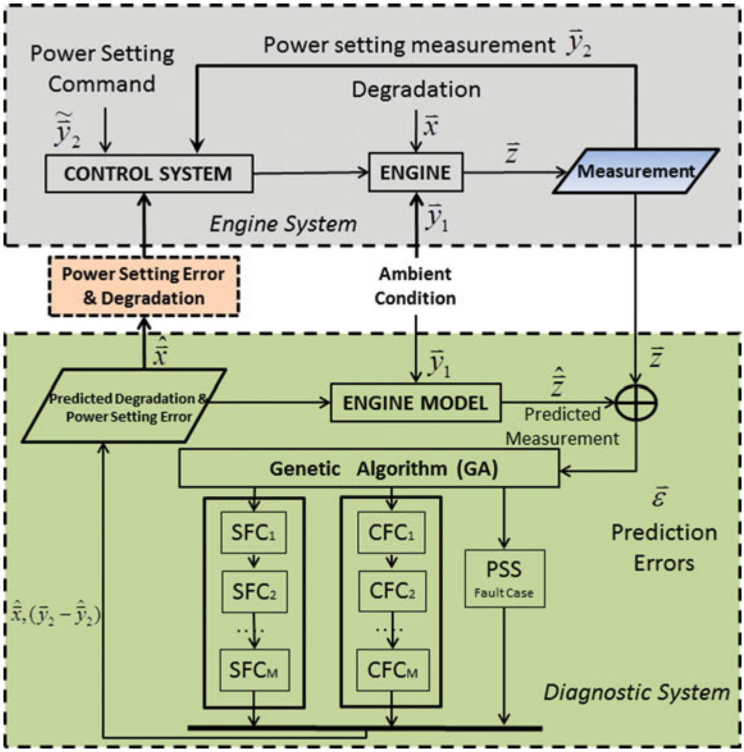

Figure 1. (Colour online) Gas turbine and its control and diagnostic systems.

of the parameters, and $h()$ represents a thermodynamic relationship among these parameters. $\vec{y}$ may include $\vec{y}_1$ representing ambient condition parameters and $\vec{y}_2$ representing the power-setting parameter shown in Fig. 1.

The engine operation may be instructed by a 'power setting command' $\tilde{\vec{y}}_2$ and controlled by an engine control system. The actual performance of the engine is indicated by the engine gas path measurements $\vec{z}$. The measured power setting parameter $\vec{y}_2$ has a direct impact on engine control and engine performance due to the fact that the control system always tries to keep the power-setting parameter to its target value based on its measurement. Therefore, any power-setting sensor (PSS) bias $(\vec{y}_2 - \tilde{\vec{y}}_2)$ will result in a shifted power setting parameter and also engine performance. This phenomenon is schematically demonstrated in Fig. 2. Of course, the engine performance is also affected by ambient condition $\vec{y}_1$ and engine degradation $\vec{x}$.

Gas turbine performance modelling is based on fundamental thermodynamics. Performance behaviour of major gas turbine components such as compressors, combustors and turbines are represented by empirical component characteristic maps that are normally obtained from component rig tests. Predictions of engine steady-state off-design and degraded performance are achieved by satisfying the continuity of mass flow and energy within engines using Newton Raphson iteration method. More details of gas turbine performance simulation can be found in Ref. 28. PYTHIA computer software[8] developed at Cranfield University for gas turbine performance simulation and gas path diagnostics is used in this study, where the diagnostic method introduced in this paper has been implemented.

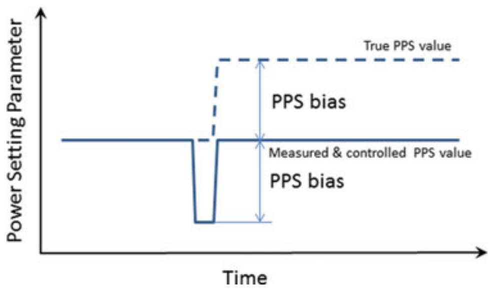

Figure 2. (Colour online) Engine controlled at constant power demand with PSS bias.

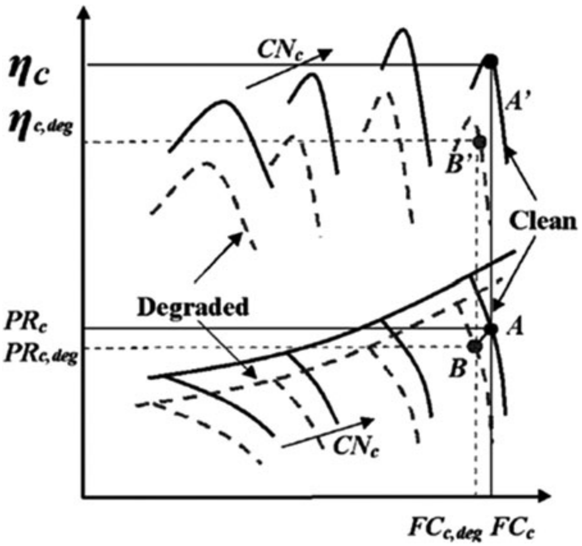

Figure 3. Compressor characteristic map [9].

2.2 Engine and sensor degradation

Gas turbine gas path component degradation results in changes of component characteristic maps, and such phenomena can be mathematically represented by scaled component maps. Take a compressor, for example; as shown in Fig. 3, the solid lines represent a clean compressor map while the dotted lines represent a degraded compressor map. It is assumed that the degraded maps of compressors, combustors and turbines keep the same shape as those of the original maps based on the fact that their geometries do not change significantly.

The scaling of the map as shown by example in Fig. 3, is represented by three degradation indices: flow capacity, isentropic efficiency and pressure ratio indices for compressors; a combustion efficiency index for burners; and flow capacity, isentropic efficiency and enthalpy-drop indices for turbines, respectively. They are defined by the ratio between the values of corresponding points on the degraded curves (dotted lines, X_B) and the original ones (solid lines, X_A)[9] in Equation (2).

$$SF = \frac{X_B}{X_A}. \tag{2}$$

https://doi.org/10.1017/aer.2017.49 Published online by Cambridge University Press

To simplify the representation of compressor degradation, it is assumed that the compressor flow capacity index is equal to that of the compressor pressure ratio index in Equation (3), based on the observation that the degradation of both pressure ratio and flow capacity result in the speed lines shifting toward the left-hand side of their original position and therefore has a similar effect on engine performance[9].

$$\boldsymbol{SF}_{c,FC} = \boldsymbol{SF}_{c,PR} \tag{3}$$

A similar assumption is applied to turbines, where it is assumed that the flow capacity degradation is equal but with an opposite sign to the enthalpy drop degradation as represented by Equation (4).

$$\boldsymbol{SF}_{t,FC} = -\boldsymbol{SF}_{t,DH} \tag{4}$$

Based on these assumptions, only two degradation indices are used to describe compressor and turbine degradations: flow capacity index (SF_{FC}) and isentropic efficiency index ($SF_{EFF.}$).

Combustor degradation is represented by one index only, which is the combustion efficiency index.

Sensor degradation can be represented by bias of measurements relative to the true values of the corresponding parameters. When a sensor has a fault, it produces a significant bias that is much larger than its measurement noise.

Gas turbine gas path component degradation will have a negative impact on engine performance, such as a drop in thrust or shaft power output, an increase in turbine entry temperature, a drop in specific fuel consumption or thermal efficiency, etc. Gas path sensor degradation normally does not have an impact on engine performance if it is only used for condition monitoring. However, if the measurements are used for engine control such as those for exhaust temperature, shaft rotation speeds, shaft power output (for industrial gas turbines only), etc., any bias of the power setting measurement may change the engine operating condition and consequently change engine performance and other gas path measurements.

Engine degradation may result in a deviation of engine performance. Such deviation may be indicated by so-called fault signature represented by the deviation of gas path measurements defined by Equation (5)

$$\frac{\Delta z_i}{z_i} = \frac{\hat{z}_i - z_i}{z_i} \tag{5}$$

where z_i is a measurement of a clean engine and $\hat{z}_i$ is the measurement of the degraded engine. Different engine degradation may result in different fault signatures; such information is used by gas path diagnostic system to detect the degradations.

2.3 GA-based gas path diagnostics

Gas path diagnostics for gas turbine engines may be regarded as an optimisation problem where a best possible solution of engine degradation is searched among all feasible solutions. Different searching or optimisation methods are available, but a genetic algorithm is used in this study due to many of its advantages described in the following. Compared with conventional optimisation methods, GAs have several distinctive features. For example, no derivatives are needed, so any non-smooth functions can be optimised; constraints can be dealt with in a very different way, such as by means of penalty functions or design of special operations; global search is used to avoid getting stuck at a local minimum; and probabilistic rather than deterministic transition rules are used to create the next generation of strings from the current one. Four operators are typically used in GAs to generate strings from one generation to the next during searching processes. More details of GAs may be found in Ref. 29. The GA operators used in this study according to 'survival of the fittest' criteria are as follows:

- Selection – select better strings from current population and keep them only as the base strings for the next generation.
- Crossover – randomly pick up pairs of strings based on crossover probabilities. It allows information exchange between the pairs of strings in the form of swapping of parts of the strings in an attempt to produce better pairs of new strings.
- Mutation – randomly pick up strings from the current population based on mutation probabilities. Random changes are introduced to part of the selected strings in an attempt to produce better new strings.
- Alienation – randomly introduce new strings into the current population.

The basic idea of such a diagnostic method for engine and sensor fault diagnostics is proposed in this paper and shown in the lower part of Fig. 1. In the approach, a gas turbine performance model representing the 'real' engine should be set up first. Then performance adaptation[30,31] may be used to make the model accurate by using available test data of the clean engine.

The engine model receives the same ambient condition $\vec{y}_1$ and measured power setting parameter $\vec{y}_2$ as that of the 'real' engine and also the predicted engine degradations to produce an initial predicted performance $\hat{\vec{z}}$. The prediction error ε shown in Equation (6) represents the difference between the actual measurements and the predicted measurements

$$\varepsilon = \sum_{i=1}^{N} \frac{1}{N} \left| \frac{\hat{z}_i - z_i}{z_i} \right| \tag{6}$$

where z_i is the actual measurements from the "real" engine and $\hat{z}_i$ the predicted measurements from the engine model. A GA fitness defined by Equation (7) represents the quality of the GA solutions. The prediction error $\vec{\varepsilon}$ is used as the feedback to the GA algorithm in order to search for better estimation of sensor and engine degradations $\hat{\vec{x}}$. In a genetic algorithm searching process, the GA fitness is maximised in order to search for the optimal estimate of engine component degradation, gas path sensor degradation and power setting sensor fault.

$$\text{Fitness} = \frac{1}{1+\varepsilon} \tag{7}$$

GA-based gas path diagnostic approach normally has a significant smearing effect in the predicted degradations if all degradations are searched simultaneously, i.e. predicted degradations may be distributed on all searched gas path components even when only few of the components or sensors are actually degraded. Such smearing effect may results in misleading diagnostic results. Therefore a component fault case (CFC) concept and sensor fault case (SFC) concept introduced in[13] are adopted in this study in order to isolate degraded components and sensors and reduce the smearing effect. In addition, a power setting sensor

https://doi.org/10.1017/aer.2017.49 Published online by Cambridge University Press

Table 1
Model engine performance specification at cruise condition (Altitude 11km and Mach number 0.8 at standard ISA condition)

Parameter	Value	Unit
Turbine entry temperature (TET)	1,480	°K
Net Thrust	78924	N
Specific Fuel Consumption (*sfc*)	26.42	g/kN.s
Air mass flow rate	150	kg/s
LPC (fan) pressure ratio	1.6	–
HPC pressure ratio	36.5	–
Bypass ratio	5.0	–

(PSS) fault case is introduced in this study to take into account the PSS fault. In other words, all potential fault cases, i.e., the combination of all potentially degraded gas path components and/or sensors, will be searched by the GA algorithm and those with high values of GA fitness would indicate most likely degraded components and/or sensors.

During the GA diagnostic searching process, CFCs, SFCs and PSS fault may be searched individually or in combinations. From practical point of view, the following considerations are recommended:

- Power setting sensor (PSS) faults should always be included in GA searching processes.
- Gas path sensor faults should be searched before gas path component faults are searched.
- The measurements of faulty gas path sensor(s) should be excluded from the measurement set for engine component fault diagnosis.

The following criteria may be used to terminate GA searching process:

(1) Maximum GA Fitness of the population exceeds 0.95

(2) Generation number exceeds 50

3.0 APPLICATION, RESULTS AND DISCUSSION

3.1 Model gas turbine engine and measurements

A model aero gas turbine engine is used in this study. It is a two-shaft turbofan engine consisting of an intake, a fan or low-pressure compressor (LPC) driven by a low-pressure turbine (LPT), a high-pressure compressor (HPC) driven by a high-pressure turbine (HPT), a combustor, a bypass nozzle and a core nozzle. The configuration of the model engine is schematically shown in Fig. 4 and its performance specification is shown in Table 1.

A performance model for the model engine was created by using Cranfield's gas turbine performance and diagnostics software PYTHIA[8] and the model configuration is graphically shown in Fig. 5.

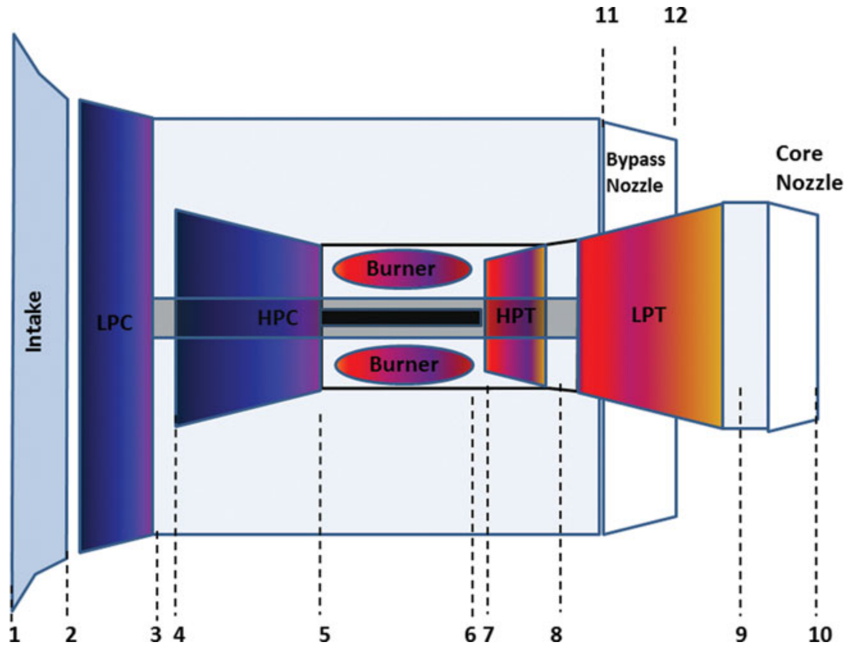

Figure 4. (Colour online) Model engine configuration.

Figure 5. (Colour online) Gas turbine performance model in PYTHIA.

It is assumed that the model engine operates at cruise condition, i.e. at altitude of 11 km and flight Mach number 0.8 at standard ISA condition, which is regarded as a nominal operating condition.

The gas path measurements of the model engine are shown in Table 2 where the gas path station numbers are shown in Fig. 4. The engine operating condition is indicated by its turbine entry temperature (TET) that is also used as the power setting parameter of the model engine. As TET cannot be directly measured due to the hostile environment, it is normally induced from engine exhaust temperature, so estimation errors or sensor bias of TET may exist.

3.2 Model engine component and sensor degradation

Although multiple gas path components and sensors may degrade simultaneously in gas turbine engines, it is assumed in this study that a power-setting sensor (PSS) fault, a gas path sensor fault and a gas path component fault may exist individually or simultaneously as typical scenarios. The assumed sensor and engine component faults are shown in Table 3 for the purpose of demonstration of the introduced diagnostic approach. The values of the sensor faults are chosen randomly with the consideration that they should be much larger than measurement noise but not so large so the fault cannot be easily spotted. These degradations are implemented into the model engine either individually or simultaneously, and the corresponding performance change and measurement samples can be simulated.

Table 2
Gas path measurements

Description	Variable
Turbine Entry Temperature (K)	TET
Fan or LPC exit total pressure (atm)	P_3
Fan or LPC exit total temperature (K)	T_3
High-pressure compressor (HPC) exit total pressure (atm)	P_5
High-pressure compressor (HPC) exit total temperature (K)	T_5
Low-pressure turbine (LPT) exit total pressure (atm)	P_9
Low-pressure turbine (LPT) exit total temperature (K)	T_9
Low-pressure shaft relative rotational speed	PCN1
High-pressure shaft relative rotational speed	PCN2
Fuel flow rate (kg/s)	m_f

Table 3
Sensor and engine degradation

Health Parameters		Value
Power-Setting Sensor (PSS) fault (i.e., TET bias) (K)		−10
Gas path sensor (P5) fault (times of maximum measurement noise)		−5
High-pressure turbine (HPT) degradation (%)	ΔEF_{HPT}	−1
	ΔFC_{HPT}	−3

3.3 Simulation of fault signatures

The samples of gas path measurements (Table 2) of a clean (i.e., un-degraded) and degraded engine are simulated by running the engine performance model with and without component degradations (Table 3) at cruise condition. Measurement noise is not included in the simulated measurement samples for simplicity. However, the impact of the measurement noise on the accuracy of diagnostic results is discussed later in this paper.

Referring to the engine and its control system shown in Fig. 1, the ‘power setting command’ requests the engine to operate at TET of 1,480°K and such a command is passed to the model engine via the control system. When a –10°K bias happens to the TET measurement, the engine control system still keeps the engine operating at measured TET of 1,480°K based on the PSS signal while the engine is actually operating at 1,490°K. Such a shift in power setting, together with HPT and P5 sensor degradation, will generate fault signatures of the engine. The fault signatures for the three fault scenarios shown in Table 4 are simulated and shown in Fig. 6. These fault signatures are crucial input for the GA-based engine and sensor fault diagnostics.

3.4 PSS fault case, CFCs and SFCs

The power-setting sensor fault has a special impact on engine performance and the diagnosis of PSS fault is also the focus of this study. Therefore it is treated as a separate type of fault case.

https://doi.org/10.1017/aer.2017.49 Published online by Cambridge University Press

Table 4
Implanted degradations in case studies

Case Study	Degradation
1	PSS (TET) bias of –10°K
2	Same PSS bias + P5 bias at the magnitude of –5 times of its maximum measurement noise
3	Same PSS bias + same P5 bias + HPT degradation (–1% efficiency degradation and –3% flow capacity degradation)

Table 5
Component fault cases (CFCs)

	Component Involved	Health Parameters	GA Search Domain (%)
CFC1	LPC	EF_{LPC} Index	(−5.0, 0.01)
		FC_{LPC} Index	(−5.0, 0.01)
CFC2	HPC	EF_{HPC} Index	(−5.0, 0.01)
		FC_{HPC} Index	(−5.0, 0.01)
CFC3	Burner	EF_{B} Index	(−5.0, 0.01)
CFC4	HPT	EF_{HPT} Index	(−5.0, 0.01)
		FC_{HPT} Index	(−5.0, 5.0)
CFC5	LPT	EF_{LPT} Index	(−5.0, 0.01)
		FC_{LPT} Index	(−5.0, 5.0)

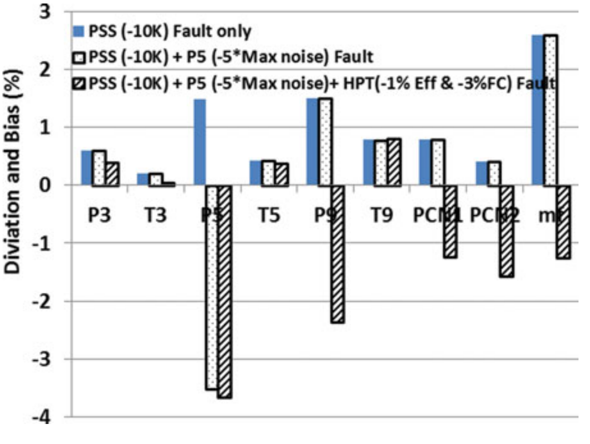

Figure 6. (Colour online) Fault signatures of three degradation scenarios.

To isolate degraded component(s) in different degradation scenarios, it is assumed that the five major gas path components – i.e. the low- and high- pressure compressors (LPC and HPC), the burner, and the high- and low-pressure turbines (LPT and HPT) – are potentially degraded components and only one of the components may degrade significantly at a time. Therefore, there are five component fault cases in total and they are shown in Table 5 where

https://doi.org/10.1017/aer.2017.49 Published online by Cambridge University Press

Table 6
Sensor fault cases (SFCs)

	Excluded Sensor		Excluded Sensor
SFC1	P3	SFC5	P9
SFC2	T3	SFC6	T9
SFC3	P5	SFC7	PCN2
SFC4	T5	SFC8	mf

Table 7
GA parameters

GA Parameter	Value
Population Size	50
Number of Generations	50
Probability of Cross-Over	0.5
Probability of Mutation	0.3
Number of Alienations	2

the health parameters and the GA searching domains for the parameters are also included. In the GA diagnostic process, each of the CFCs is searched and the CFCs with high values of GA fitness are most likely to be true.

Similarly, sensor fault cases are identified in order to isolate and detect gas path sensor faults. It is assumed that only one gas path sensor may fail at a time. Therefore each SFC includes all sensors listed on Table 2 except one; these SFCs and the excluded sensors in individual SFCs are listed on Table 6.

3.5 GA parameters

To carry out the GA diagnostic searching process based on Fig. 1, the most important GA parameters and their values are identified and shown in Table 7. The selection of the values of the GA parameters is a compromise between the searching accuracy and the speed of GA calculations. Trial and error may be used to find the best values for the parameters.

3.6 Case study 1: Diagnosis of PSS degradation

In this case study, it is assumed that only the PSS bias of –10°K happens and no other gas path sensor and engine component faults exist.

If no sensor faults are considered, the diagnostic analysis may only focus on engine gas path components. In other words, all CFCs defined in Table 5 may be searched and the results are shown in Fig. 7 marked as 'Exclude PSS fault'. It can be seen that the GA Fitness for all component fault cases are very low, between 0.4 and 0.6. This indicates that the obtained CFC results are not correct and the searching for degradation fails.

If the PSS fault is included, the above searching process is repeated and the results are also shown on Fig. 7 marked as 'Include PSS fault'. It can be seen that the obtained GA fitness are much higher (around 0.9 for all CFCs), indicating that the actual degradation may very likely have been found in the obtained results. By comparing the predicted degradation with

https://doi.org/10.1017/aer.2017.49 Published online by Cambridge University Press

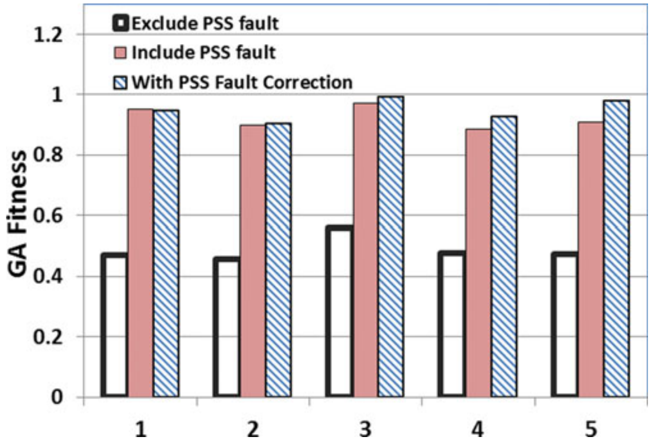

Figure 7. (Colour online) GA fitness of CFCs with and without inclusion of PSS fault in case study 1.

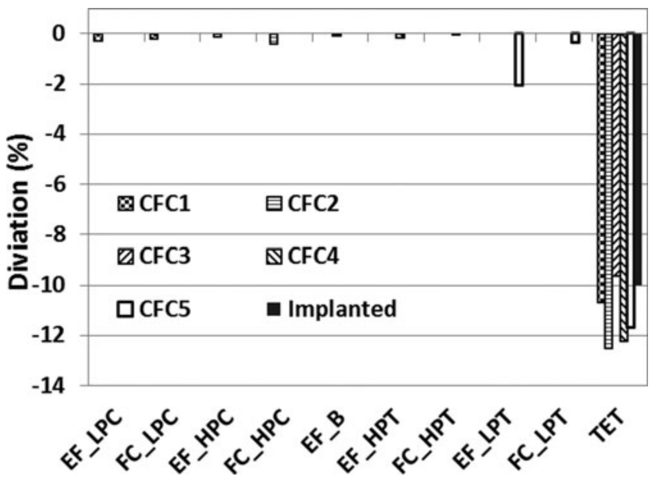

Figure 8. Predicted engine component and PSS faults in case study 1.

the implanted degradation in Fig. 8, it can be seen that the PSS fault has been predicted quite satisfactorily with a small smearing effect on the LP turbine.

Based on the results shown in Fig. 8, it can be concluded that the PSS has a fault and the PSS bias may be between –9°K and –13°K and there is a possibility of LP turbine degradation. Based on such analysis, –10°K PSS bias is corrected and all the CFCs are searched again. The corresponding results are shown on Figs 7 and 9 marked as 'With PSS fault correction'. It is obvious at this time that the GA fitness for all CFCs is close to 1.0, and the predicted component degradations are very small and can be ignored. It clearly indicates that the true degradation happens at PSS only and no engine components degrade.

3.7 Case study 2: Diagnosis of PSS and P5 sensor degradation

In this case study, it is assumed that PSS has a bias of –10K and P5 has a bias of –5 times of its maximum measurement noise level. Both faults are implemented into the engine model and the fault signature is shown on Fig. 6 marked as 'PSS (–10°K) +P5 (-5 · Max noise) fault'.

https://doi.org/10.1017/aer.2017.49 Published online by Cambridge University Press

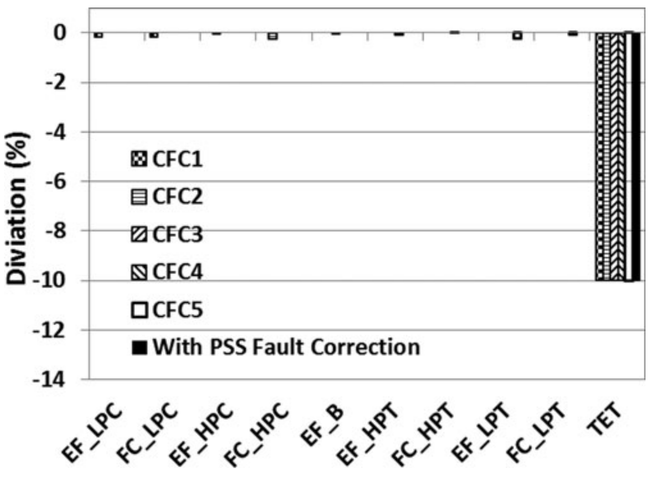

Figure 9. Predicted engine component degradation with PSS fault correction included in case study 1.

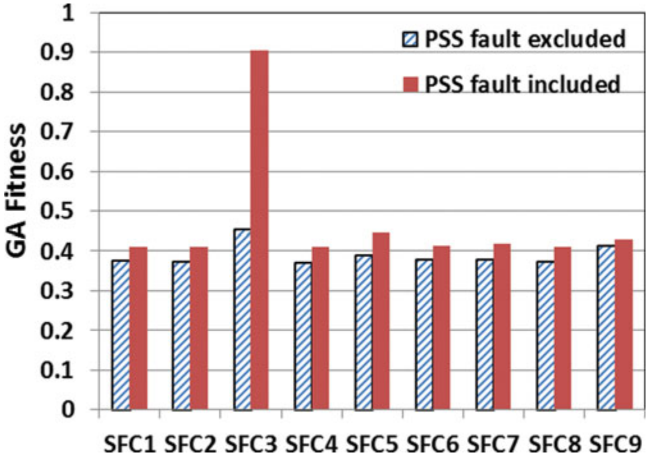

Figure 10. (Colour online) GA fitness of case study 2.

Sensor fault detection is normally done before engine gas path component diagnostics. If it is assumed that the PSS has no fault, all eight single SFCs shown in Table 6 may be searched and the results are shown in Fig. 10. It can be seen that GA fitness for all SFCs are around 0.35 and 0.45, regarded as low values. This indicates that the search for sensor faults has failed.

By including the PSS fault in the GA search, all SFCs have been searched again and the corresponding GA fitness for all SFCs is shown on Fig. 10. It can be seen that the GA fitness for most of the SFCs is around 0.4 and SFC3 shows exceptionally high value of GA Fitness, around 0.9. Such results indicate that the true gas path sensor fault may very likely happen on P5. Further results of the predicted PSS biases for all SFCs as seen in Fig. 11 show that the predicted PSS bias of SFC3 is around –12.2°K, quite close to the true value of the PSS bias of –10°K. The predicted PSS biases of other SFCs are regarded as not true due to corresponding low GA fitness.

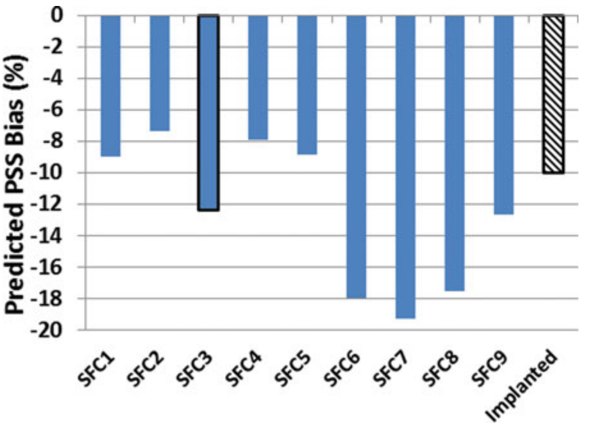

Figure 11. (Colour online) Predicted PSS bias in case study 2.

3.8 Case study 3: Diagnostics of PSS, P5 and HPT degradation

A more complicated degradation case is demonstrated here where PSS, P5 and the HPT are degraded simultaneously, and the fault signature of this case is shown in Fig. 6.

To include all three types of degradations in the diagnostic analysis, the following should be considered:

- PSS fault case should be included in all GA diagnostic searches.
- Gas path SFCs should be searched first to detect and exclude a faulty gas path sensor.
- During the SFC search, a CFC has to be chosen randomly and searched simultaneously with SFCs.

Based on the above, the randomly chosen CFC may refer to an un-degraded component (such as HPC in CFC2) or the degraded component (such as HPT in CFC4) as the actually degraded engine component is unknown.

To demonstrate the difference between choosing an un-degraded component and the degraded component for sensor fault detection, two examples of the search results of all SFCs are shown in Fig. 12 where one refers to choosing CFC2 (HPC) and the other refers to choosing CFC4 (HPT). It can be seen in the first example that the GA fitness for all SFCs has low values of around 0.4 except SFC3, which has a GA fitness of around 0.9 referring to the P5 sensor. When the degraded component HPT (CFC4) is chosen in the second example, the GA fitness for most of the SFCs increase to around 0.65, except SFC3 (P5) and SFC4 (T5) have a GA fitness close to 1.0. The increase of the average GA fitness is expected as the actually degraded component HPT is included in the GA search. The faulty P5 sensor is correctly picked up in SFC3, while unfortunately the high GA fitness for SFC4 is unexpected, as T5 is not faulty. To understand the reasons for the high value of GA fitness for SFC4, further analysis was carried out and the details are given in the following.

By looking at the details of the predicted degradations in the two examples and a comparison with the implanted degradation shown in Table 8, the predictions from CFC4 + SFC3 are very satisfactory, but the predicted degradations from CFC4 + SFC4 are very different compared with those of the implanted fault. Further analysis reveals that when T5

https://doi.org/10.1017/aer.2017.49 Published online by Cambridge University Press

Table 8
Predicted degradation in case study 3

	GA Fitness	TET Bias (°K)	EF_HPT (%)	FC_HPT (%)
CFC4+SFC3	0.996	− 9.92	− 0.99	− 2.98
CFC4+SFC4	0.926	1.45	− 0.87	1.32
Implanted	n/a	−10	− 1.0	− 3.0

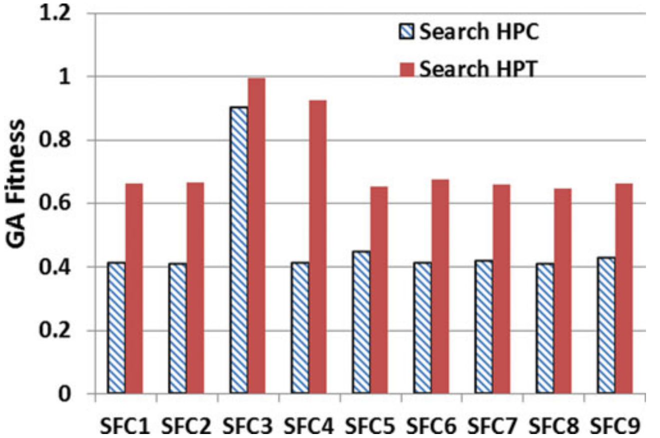

Figure 12. (Colour online) Predicted GA fitness in case study 3.

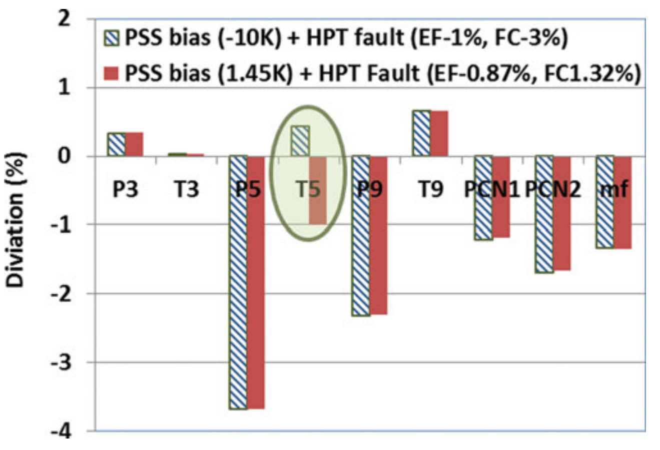

Figure 13. (Colour online) Comparison of PSS and HPT fault signatures.

is excluded in SFC4, a combination of PSS (TET) bias of 1.45°K and a HPT degradation (−0.87% degradation in efficiency index and 1.32% degradation in flow capacity index) produce almost an identical fault signature to that of the implanted degradation as shown in Fig. 13. This indicates that T5 is so important in the diagnostic analysis that if the T5 sensor is excluded, misleading diagnostic results may be predicted. In other words, the T5 sensor and

https://doi.org/10.1017/aer.2017.49 Published online by Cambridge University Press

Table 9
Range of prediction uncertainties

	Due to GA Stochastics	Due to GA Stochastics & Measurement Noise
HPT EF Index (%)	0.04	0.25
HPT FC Index (%)	0.54	2.02
TET (K)	1.83	8.43

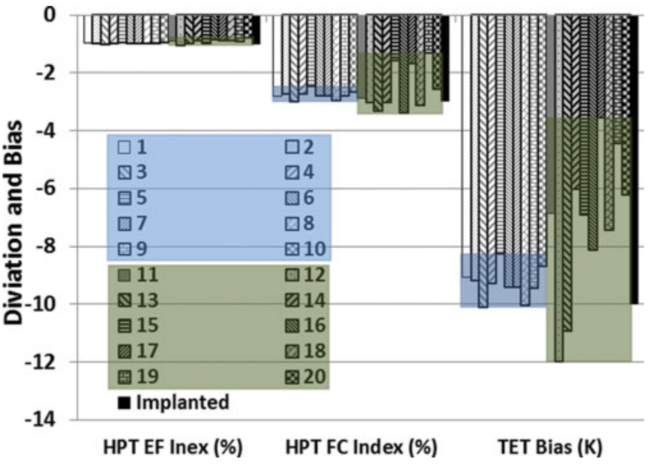

Figure 14. (Colour online) Predicted degradation from repeated GA search of CFC4 + SFC3 with and without measurement noise in case study 3.

HPT degradation can be misdiagnosed in such a complicated degradation scenario, which may be inevitable.

3.9 Case study 4: Prediction uncertainties

There are two major factors that may result in reduced accuracy of the GA diagnostic predictions; one is the GA approach itself due to its stochastic nature, and the other is the impact of measurement noise.

The prediction uncertainties are investigated by running 10 repeated GA searches of CFC4 + SFC3 in Case Study 3 and comparing the results marked as 1–10 in Fig. 14. The range of prediction uncertainties due to GA stochastics are shown in Table 9 where the variations of the efficiency (EF) index and the flow capacity (FC) index are within 0.04% and 0.54% respectively, and the variation of the TET bias is within 1.83°K, which is quite small.

Measurement noise is inevitable in real life and will have a negative impact on diagnostic results. To analyse the impact of measurement noise on diagnostic errors, a measurement noise model with the maximum levels of measurement noise shown in Table 10 is implemented into measurement simulations. The measurement noise is randomly generated following Gaussian-type distribution and is imposed on the true values of the simulated gas path measurements to generate multiple samples. In this study, 10 sets of random samples are generated and

https://doi.org/10.1017/aer.2017.49 Published online by Cambridge University Press

Table 10
Maximum measurement noise [32]

Measurement	Range	Typical Error
Pressure	3–45 psia	±0.5%
	8–460 psia	±0.5% or 0.125 psia whichever is greater
Temperature	−65–290°C	± 3.3 °C
	290–1000°C	$\pm\sqrt{2.5^2 + (0.0075 \cdot T)^2}$
	1000–1300°C	$\pm\sqrt{3.5^2 + (0.0075 \cdot T)^2}$
Fuel Flow	Up to 250 kg/hr	41.5 kg/hr
	Up to 450 kg/hr	34.3 kg/hr
	Up to 900 kg/hr	29.4 kg/hr
	Up to 1360 kg/hr	23.7 kg/hr
	Up to 1815 kg/hr	20.8 kg/hr
	Up to 2270 kg/hr	23.0 kg/hr
	Up to 2725 kg/hr	25.9 kg/hr
	Up to 3630 kg/hr	36.2 kg/hr
	Up to 5450 kg/hr	63.4 kg/hr
	Up to 12260 kg/hr	142.7 kg/hr

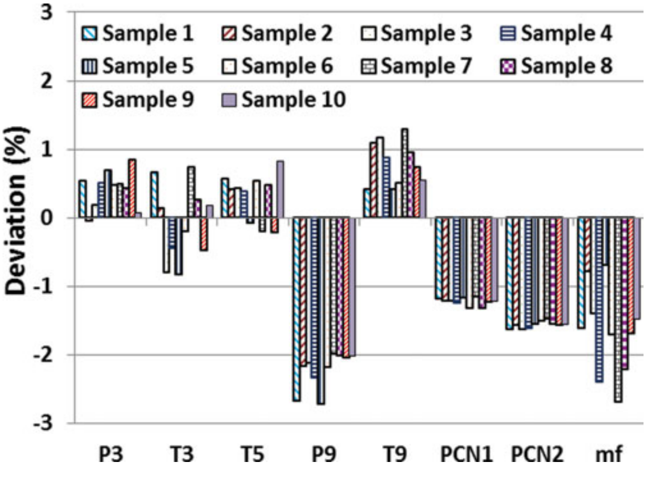

Figure 15. (Colour online) Fault signatures inclusive of measurement noise.

the corresponding fault signatures are shown in Fig. 15 showing that the fault signatures are slightly different.

The GA diagnostic searching process (Fig. 1) is applied to the search of CFC4 + SFC3 using the 10 fault signatures shown in Fig. 15 with the inclusion of PSS fault case. Consequently, the obtained GA fitness values of the 10 results are shown on Fig. 16 (points 11–20) and the predicted HPT degradation and the PSS bias are shown in Fig. 14 (numbered from 11–20). Compared with similar results shown in Fig. 16 where no measurement noise is considered, it can be seen that the average GA fitness drops from around 0.94–0.99 to around

https://doi.org/10.1017/aer.2017.49 Published online by Cambridge University Press

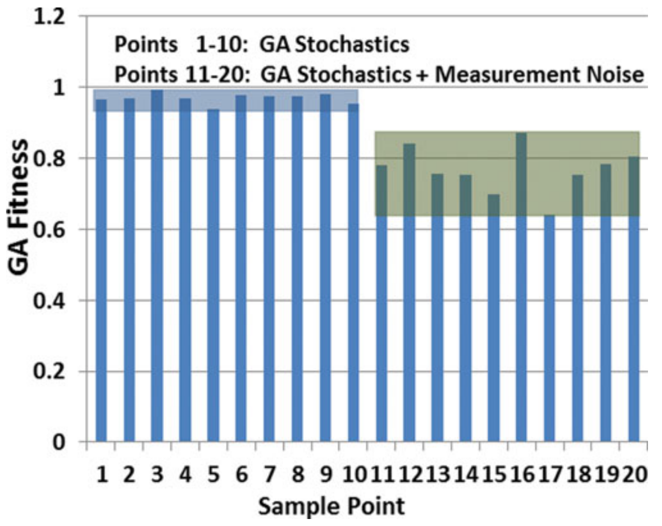

Figure 16. (Colour online) GA fitness from repeated GA search inclusive of measurement noise: CFC4 + SFC3 in case study 3.

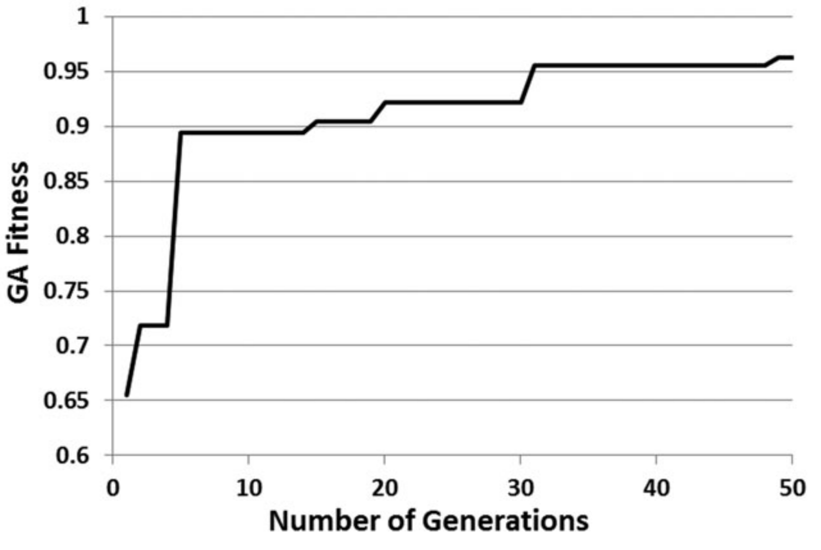

Figure 17. GA searching process – fitness vs number of generations.

0.64–0.87, i.e., becoming lower and having greater scattering. The prediction uncertainties of the health parameters also become larger as shown in Fig. 14 and Table 9. In other words, the prediction uncertainties increase from 0.04% to 0.25% for HPT FC index, from 0.54% to 2.02% for HPT FC index, and from 1.8°K to 8.4°K for TET bias.

3.10 Speed of calculations

A typical convergence process is shown in Fig. 17 where the maximum Fitness of the population varies with the GA generation number. It takes about 18 seconds for a generation

https://doi.org/10.1017/aer.2017.49 Published online by Cambridge University Press

and about 15 minutes to get a solution based on the GA setting shown on Table 7 using a typical desktop computer with a duo Intel Core i7-3770 processor and 3.4 GHz CPU. Such a calculation is relatively slow compared with other gas path diagnostic methods and is only suggested for off-line diagnostic analysis.

3.11 Applicability of diagnostic approach

Although gas turbine engines may have slightly different configurations, they all have similar components, work following a similar principle, have similar gas path measurements and are controlled in a similar way by using a power setting parameter. Therefore, the gas path diagnostic method introduced in this paper for gas turbine power setting sensor, gas path sensors and gas path components has no limitations in theory to be applied to any other gas turbine engines.

4.0 CONCLUSIONS

In this paper, a GA-based gas path diagnostic approach for gas turbine power-setting sensor faults with or without the existence of gas path component degradation and a gas path sensor fault has been proposed. The developed diagnostic approach has been applied to the diagnostic analysis of a model aero turbofan engine where the degradation of the power-setting sensor, the high-pressure turbine and total pressure sensor at the exit of the high-pressure compressor is assumed to have happened. The diagnostic results of three case studies for the model engine show that:

- The PSS fault will shift the whole gas turbine performance. Without the inclusion of the PSS fault case, the GA diagnostic approach is not able to perform properly when the PSS fault happens.
- The introduced GA diagnostic method is able to detect power setting sensor fault successfully with and without the existence of single component fault (such as HPT degradation) and single gas path sensor fault (such as a P5 fault).
- The PSS fault may result in a fault signature similar to that of component degradation in exceptional situations, which may cause difficulties in identifying the true degradation
- Both GA stochastics and measurement noise have a negative impact on diagnostic accuracy. Case studies show that there are up to 0.04%, 0.54% and 1.83°K prediction uncertainties for HPT EF index, HPT FC index and TET bias respectively due to GA stochastics, and up to 0.25%, 2.02% and 8.4°K prediction uncertainties for the same health parameters respectively due to both GA stochastics and measurement noise.
- The computing speed of the GA-based diagnostic approach is relatively low compared to other gas path diagnostic methods. It takes about 15 minutes of computing time to get a solution using a typical desktop computer, which may only be suitable for off-line diagnostic applications.
- In theory, such diagnostic method can be applied to different gas turbine engines.

REFERENCES

1. LI, Y.G. Performance-analysis-based gas turbine diagnostics: a review, *Proceedings of the Institution of Mechanical Engineers, Part A: J. Power and Energy*, 2002, **216**.

2. Singh, R. Advances and opportunities in gas path diagnostics, ISABE-2003-1008, ISABE, 2003, Cleveland, Ohio, US.
3. Jaw, L.C. Recent advances in aircraft engine health management (EHM) technologies and recommendations for the next step, GT2005-68625, ASME Turbo Expo, 2005, Reno, Nevada, US.
4. Urban, L.A. Gas path analysis applied to turbine engine condition monitoring, AIAA 72–1082, AIAA/SAE 8th Joint Propulsion Specialist Conference, 1972, New Orleans, Louisiana, US.
5. Doel, D.L. An assessment of weighted-least-squares-based gas path analysis, *J Engineering for Gas Turbines and Power*, 1994, **116**, (2).
6. Volponi, A.J. Gas path analysis: An approach to engine diagnostics, 35th Symposium of Mechanical Failures Prevention Group,1982, Gaithersburg, Maryland, US.
7. Provost, M.J. COMPASS: A generalized ground-based monitoring system, *AGARD-CP-449*, 1988.
8. Li, Y.G. and Singh, R. An advanced gas turbine gas path diagnostic system – PYTHIA, ISABE-2005-1284, 2005, ISABE, Munich, Germany.
9. Li, Y.G. Gas turbine performance and health status estimation using adaptive gas path analysis, *J Engineering for Gas Turbines and Power*, 2010, **132**, (4).
10. Denney, G. F16 jet engine trending and diagnostics with neural networks, *Proceedings of the SPIE*, 1993, **1965**.
11. Ogaji, S.O.T. and Singh, R. Gas path fault diagnosis framework for a three-shaft gas turbine, *J Power and Energy*, 2003, **217**.
12. Tan, H.S. Fourier neural networks and generalized single hidden layer networks in aircraft engine fault diagnostics, *J of Engineering for Gas Turbines and Power*, 2006, **128**, (4).
13. Zedda, M. and Singh, R. Gas turbine engine and sensor fault diagnosis using optimization techniques, *J Propulsion and Power*, 2002, **18**, (5).
14. Gulati, A., Zedda, M. and Singh, R. Gas turbine engine and sensor multiple operating point analysis using optimization techniques, *AIAA 2000–3716, AIAA/ASME/SAE/ASEE Joint Propulsion Conference & Exhibit*, Huntsville, Alabama, US, 2000.
15. Wallin, M. and Grönstedt, T. A comparative study of genetic algorithms and gradient methods for RM12 turbofan engine diagnostics and performance estimation, GT2004-53591, ASME Turbo Expo, 2004, Vienna, Austria.
16. Ganguli, R. Application of fuzzy logic for fault isolation of jet engines, 2001-GT-0013, ASME Turbo Expo, 2003, New Orleans, Louisiana, US.
17. Martis, D. Fuzzy logic estimation applied to newton methods for gas turbines, *J Engineering for Gas Turbines and Power*, 2007, **129**, (1).
18. Eustace, R. A real-world application of fuzzy logic and influence coefficients for gas turbine performance diagnostics, *J Engineering for Gas Turbines and Power*, 2008, **130**, (6).
19. Romessis, C. and Mathioudakis, K. Bayesian network approach for gas path fault diagnosis, *J Engineering for Gas Turbines and Power*, 2006, **128**, (1).
20. Li, Y.G. A gas turbine diagnostic approach with transient measurement, *J Power and Energy*, 2003, **217**.
21. Surender, V.P. Adaptive myriad filter for improved gas turbine condition monitoring using transient data, *J Engineering for Gas Turbines and Power*, 2005, **127**, (2), 2005.
22. Ogaji, S.O.T., Singh, R. and Probert, S.D. Multiple-sensor fault diagnoses for a 2-shaft stationary gas turbine, *Applied Energy*, 2002, **71**, pp 321-339.
23. Romesis, C. and Mathioudakis, K. Setting up of a probabilistic neural network for sensor fault detection including operation with component faults, *J Engineering for Gas Turbines and Power*, 2003, **125**, pp 634-641.
24. Palme, T., Fast, M. and Thern, M. Gas turbine sensor validation through classification with artificial neural networks, *Applied Energy*, 2011, **88**, (11), pp 3898-3904.
25. Aretakis, N., Mathioudakis, K. and Stamatis, A. Identification of sensor faults on turbofan engine using pattern recognition techniques, *Control Engineering Practice*, 2004, **12**, pp 827-836.
26. Mehranbod, N., Soroush, M. and Panjapornpon, C. A method of sensor fault detection and identification, *J Process Control*, 2005, **15**, (3), pp 321-339.
27. Courdier, A. and Li, Y.G. Power setting sensor fault detection and accommodation for gas turbine engines using artificial neural networks, ASME GT2016-56304, Turbo Expo, 2016.
28. MacMillan, W. Development of a Modular Type Computer Program for the Calculation of Gas Turbine Off Design Performance, PhD thesis, 1974, Cranfield Institute of Technology.

29. MICHALEWICZ, Z. *Genetic Algorithms + Data Structures = Evolution Programmes*, 3rd ed, Springer-Verlag Berlin Heidelberg, Germany, 1999.
30. LI, Y.G., PILIDIS, P. and NEWBY, M. An adaptation approach for gas turbine design-point performance simulation, *J of Engineering for Gas Turbine and Power*, October 2006, **128**, pp 789-795.
31. LI, Y.G., ABDUL GHAFIR, M.F., WANG, L., SINGH, R., HUANG, K., FENG, X. and ZHANG, W. Improved multiple point non-linear genetic algorithm based performance adaptation using least square method, *J Engineering for Gas Turbines and Power*, March 2012, **134**, pp 031701.
32. DYSON, R.J.E. and DOEL, D.L. CF-80 condition monitoring – the engine manufacturing's involvement in data acquisition and analysis, AIAA-84-1412, 1987.

https://doi.org/10.1017/aer.2017.49 Published online by Cambridge University Press